11th Australasian Fluid Mechanics Conference
University of Tasmania, Hobart, Australia
14-18 December 1992

LAMINAR FLOWS OF HIGH ENTHALPY AIR IN A COMPRESSION CORNER

S.G. MALLINSON, S.L. GAI and N.R. MUDFORD

Department of Mechanical Engineering, University College
Australian Defence Force Academy
Campbell, ACT 2600, AUSTRALIA

ABSTRACT

Laminar flows of high enthalpy air in a flat plate-ramp compression corner have been experimenatlly investigated using a free-piston shock tunnel. The data for the ramp set at zero degrees incidence agrees with previuosly obtained flat plate data. The heat transfer distributions for separated flows exhibit a diffuse reattachment process and have a smaller separated region than perfect gas flows. This is explained by the fact that the kinetic energy for the high enthalpy flows is lower due to dissociation which lowers the viscosity and thus extent of the separated region.

1. INTRODUCTION

Compression corners are a frequently encountered feature on the control surfaces and in the inlet regions of re-entry vehicles (Figure 1). The pressure rise due to the ramp induced shock wave is transmitted upstream via the subsonic portion of the boundary layer. For sufficiently high compression angles, this shock wave / boundary layer interaction will cause the boundary layer to detach from the surface. The boundary layer is forced to reattach on the face of the ramp. Such separation and reattachment can alter the pressure and heat transfer distributions over the vehicle thus affecting the control effectiveness and the performance of the propulsion systems. Hypersonic laminar compression corner flows have been extensively studied for the case of a perfect gas, both experimentally and theoretically. Even though the enthalpies associated with re-entry flight are often sufficient for real gas phenomenon to be present, real gas effects on separation and reattachment have not been studied in great detail (Park, 1990). It is the purpose of this paper to experimentally investigate real gas effects, if any, on laminar separation and reattachment in compression corner flow.

Holden and Moselle (1970) presented flat plate-wedge data alongside results from curved compression corner experiments. These data have been used extensively as a test case for computational fluid dynamics (CFD) code validation (see, for example, Hung and MacCormack (1976) or Rudy et al (1991)) and will be used here for comparison purposes.

2. EXPERIMENTAL PROCEDURE

The experiments were performed using the Australian National University's free-piston shock tunnel, T3. A review of the operation and performance of T3 has been given by Stalker (1972). A conical nozzle was used to expand the gas. The thermodynamic and gasdynamic properties can be calculated using a nozzle flow code, such as the one known as NENZF (Lordi et al (1966)). Several detailed investigations have shown this code correctly predicts the nozzle flow conditions (Stalker, 1985). The streamwise variation of temperature and density are presented in Figure 2. The reference position for the flow was at the nozzle exit. The conditions at the nozzle exit are presented in Table 1.

The compression corner model with unit aspect ratio was manufactured from mild steel. It consisted of a flat plate and

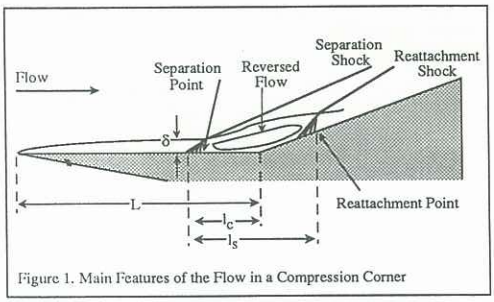

Figure 1. Main Features of the Flow in a Compression Corner

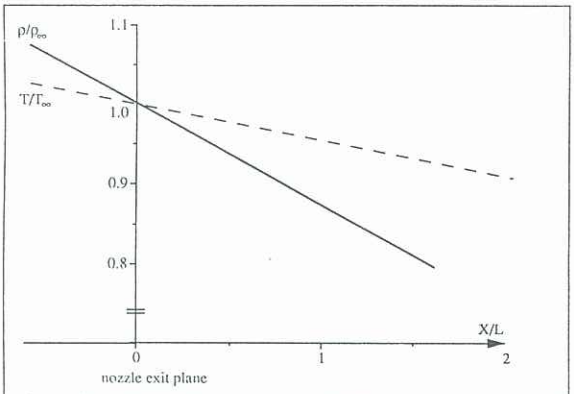

Figure 2. Streamwise Gradients for Density and Temperature. L is the flat plate length.

adjustable ramp plate, the plates being mounted upon a housing for the wires which in turn was attached to a sting (Figure 3). The leading edge was situated at the centre of the nozzle exit at recoil. The surface of the flat plate was set parallel to the centre-line axis. The sides of the model were inclined to the angle subtended by the nozzle's effective source. The heat transfer measurements were performed using chromel-alumel thermocouple gauges (Figure 4). The signals from the thermocouples were amplified and digitized before being directed to a computer for analysis. Heat transfer, q_w, was calculated from the variation of temperature with time using

$$q_w(t_n) = \frac{2}{\sqrt{\pi}}(\rho c k)^{1/2}\left[\sum_{j=1}^{n}\frac{T(t_i) - T(t_{i-1})}{(t_n - t_i)^{1/2} + (t_n - t_{i-1})^{1/2}}\right] \quad (1)$$

where t is the time, $(\rho ck)^{1/2}$ is the thermal product, T is the temperature, and the subscripts refer to the discrete points in the temperature trace. Typical surface temperature and heat transfer signals for separated flow are presented in Figure 5. Also shown in Figure 5 is a typical stagnation pressure trace. The model was tested under three different conditions designated B, D and G (Table 1). The conditions are

Condition	h_o (MJkg^{-1})	p_o (MPa)	T_o (K)	p_∞ (kPa)	T_∞ (K)	ρ_∞ (x10^3 kgm^{-3})	u_∞ (kms^{-1})	M_∞	Re_∞ (x10^{-5} m^{-1})	α_N	α_O
B	19.1	21.6	8400	0.99	1170	2.64	5.47	7.4	3.11	0.00	0.80
D	13.7	21.7	7200	1.01	950	3.45	4.72	7.5	4.05	0.00	0.43
G	2.85	22.6	2400	0.77	160	16.5	2.29	9.0	33.1	0.00	0.00

Table 1. Flow Conditions. Stagantion conditions are denoted by o, free stream conditions at the nozzle exit are denoted by ∞.

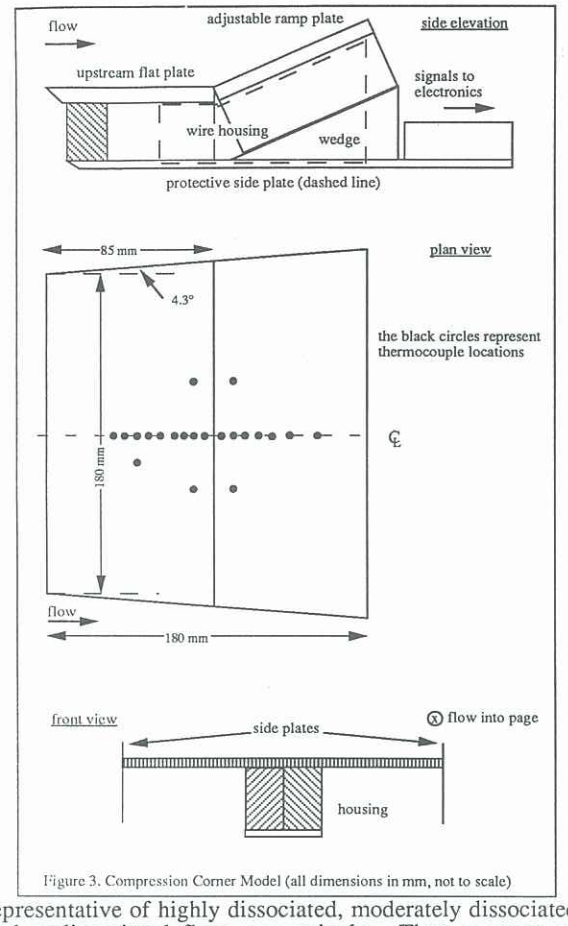

Figure 3. Compression Corner Model (all dimensions in mm, not to scale)

representative of highly dissociated, moderately dissociated and undissociated flow, respectively. Thus, a range of chemical activity was experienced.

3. RESULTS AND DISCUSSION

3.1 Flow Quality Considerations

3.1.1 Establishment of Separated Flows. The time available for measurements in a free-piston shock tunnel is limited by the shock tube sidewall shock-boundary layer interaction which can result in the early arrival of Helium in the test section (Crane and Stalker, 1977). The time required for the establishment of a steady state in a perfect gas flow is dependant upon either the time required for the passage of an acoustic wave along the surface to the edge of the separated region (Holden, 1971) or upon the characteristic values of Stanton number, velocity and boundary layer thickness (Rom, 1967). It has been shown that establishment times for real gas flows are determined by the same mechanisms and that there is sufficient time for the establishment of steady separated flows in a free-piston shock tunnel (Mallinson and Gai, 1992). This is clearly indicated by Figure 6.

3.1.2 Three-Dimensional Effects. The flow was assumed to be two-dimensional, a fact that could only be checked a priori. Sixteen thermocouples were place along the model centre line. Thermocouples were placed off the centre line but adjacent to some of the centre line devices to monitor any three-dimensional effects (Figure 3). Figure 7(a) shows the heat transfer traces for two points within the separated region,

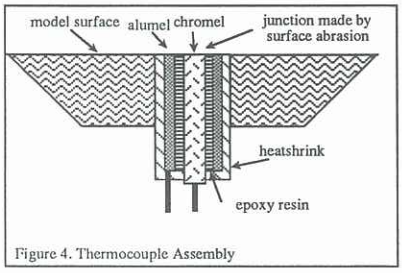

Figure 4. Thermocouple Assembly

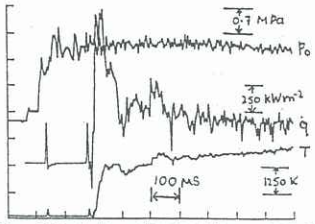

Figure 5. Typical traces for stagnation pressure, and for temperature and heat transfer in separated flow.

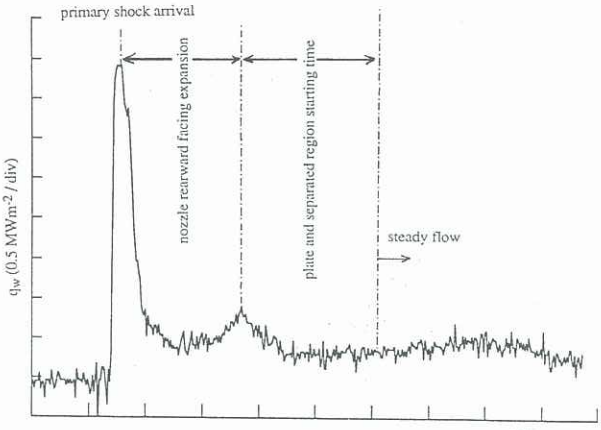

Figure 6. Typical heat transfer trace for separated flow

upstream of the corner. There are some small variations between the traces during the establishment of steady flow. Once a steady state has been reached, however, the traces are almost identical, from which it may be inferred that the flow was two-dimensional. The comparison is repeated in Figure 7(b) for flow without side fences, where again it appears that three-dimensional effects are not present. It was supposed that the outflow would produce noticeable three-dimensional effects. This is not apparent from the heat transfer traces.

3.2 Heat Transfer Distributions

A variety of ramp angles were tested for each flow condition. The angle required to provoke separation for a given free-stream Mach number, M_∞ and Reynolds number based on the upstream plate length, Re_L, is given by (Hanky, 1967, Ball, 1967),

$$M_\infty \alpha_i = \lambda \bar{\chi}_L^{1/2} \qquad (2)$$

where α_i is the ramp angle required to provoke separation, λ is a constant dependant upon the wall to total temperature ratio and $\bar{\chi}_L = M_\infty^3 \sqrt{\frac{C^*}{Re_L}}$, where C^* is the Chapman-Rubesin

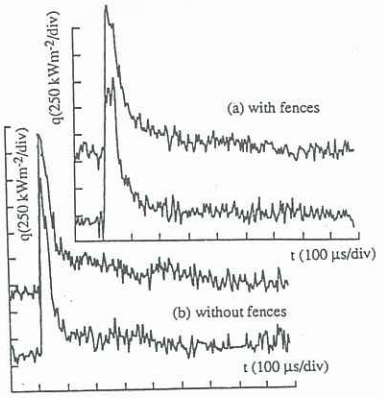

Figure 7. Heat transfer traces for thermocouples at the same displacement from the leading edge, but at different displacements from the model centre-line.

constant. For the present flow conditions, $\lambda = 1.3$ (Ball, 1967). This equation predicts that ramp angles of approximately 16°, 14° and 10° are required to provoke separation for conditions B, D and G respectively. Thus it was decided to perform experiments for ramp angles of 0° (flat-plate flow), 5°, 10°, 14°, 16°, 18° and 24°. Data from 10° and 14° are not presented herein.

3.2.1 Flat-Plate Heat Transfer. East et al (1980) performed heat transfer measurements in high enthalpy laminar flat-plate boundary layer flows. As these experiments were undertaken in the T3 facility, it is worthwhile to compare their data to that obtained in this investigation when the ramp is set at zero degrees incidence. The heat transfer data is presented in terms of Stanton number, St, defined as

$$St = \frac{q_w}{\rho_e u_e [(h_r)_{eq} - h_w]} \qquad (3)$$

where q is heat transfer, ρ is the density, u is the velocity and h is the enthalpy and the subscripts w refers to flow quantities at the walls, e refers to flow external to the boundary layer, r refers to a reference condition and eq refers to a quantity being evaluated assuming equilibrium chemistry, as was assumed by East et al when they evaluated h_r. In that situation, h_r has the form

$$h_r = (h_r)_{eq} = h_s + \tfrac{1}{2}(\sqrt{Pr}-1)u_e^2 \qquad (4)$$

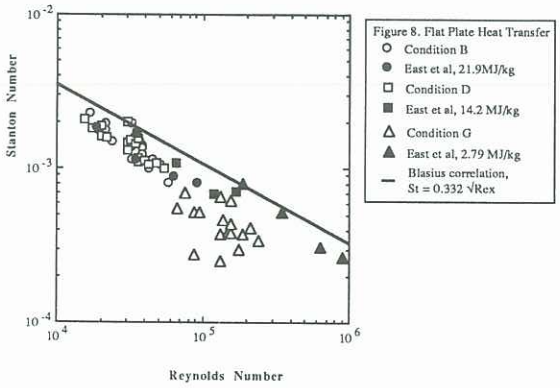

Figure 8. Flat Plate Heat Transfer

where h_s is the stagnation enthalpy and Pr is the Prandtl number. Accordingly, this assumption has been retained in the present analysis. Stanton number is plotted versus Reynolds number in Figure 8, where Reynolds number is based on the distance from the leading edge, x. That is,

$$Re_x = \frac{\rho_e u_e x}{\mu_e} \qquad (5)$$

where μ_e is the viscosity in the free-stream extrenal to the boundary layer. The present data compare favourably with the data of East et al and the simple Blasius boundary layer correlation, $St = 0.332\sqrt{Re_x}$.

3.2.2 Heat Transfer for Ramp Set at Incidence. The incidence of the ramp plate was varied by inserting wedges beneath the wire housing. Careful adjustment was required to obtain sharp, airtight corners. Packing material was placed beneath the corner to ensure that there was no airflow into the housing. The data from flows with the ramp plate set at 5°, 16 °, 18°, and 24° incidence are presented in Figures 9-12, respectively. The Stanton number has been multiplied by $\sqrt{Re_L}$ and plotted versus X/L where X is the distance from the leading edge. This permits comparison between data from different flow conditions, in a manner similar to Figure 8. Also presented in Figure 10-12 are the perfect gas data of Holden and Moselle (1970) and the results from the numerical calculation by Rudy et al (1991). The data from these two investigations pertain to 15°, 18° and 24°. The difference between 15° and 16° is expected to be only slight, with the overall features of the flow being comparable. The 5° data have a noticeably inflected minimum which corresponds to unseparated flow (Needham, 1965). The scatter in data for condition G is due to the poor signal to noise ratio experienced at low temperatures. The data for conditions B and D at 16° have a more rounded minimum corresponding to incipient separation, that is the flow is just about to separate (Needham, 1965). The data for condition G are less scattered and exhibit a peak at reattachment. The Holden and Moselle data and the numerical result are for unseparated flow. Therefore the sharp peak in heat transfer is not present.

As the ramp incidence is further increased to 18° and 24°, the region of minimum heat transfer spreads, corresponding to growth of the separated domain. For conditions B and D, the distributions show a sharp rise near reattachment followed by a gradual decay along the ramp face. This is in contrast to the peaked maximum and rapid decay after reattachment that is observed for condition G, the Holden and Moselle data and the numerical result. The reattachments for conditions B and D occur upstream of the reattachment positions observed in the other flows. This indicates a smaller separated length for the dissociated flows than that for the undissociated flows. This may be explained by the fact that for conditions B and D, some of the kinetic energy has been converted to chemical energy which results in a lower temperature and hence viscosity in the boundary layer. As the

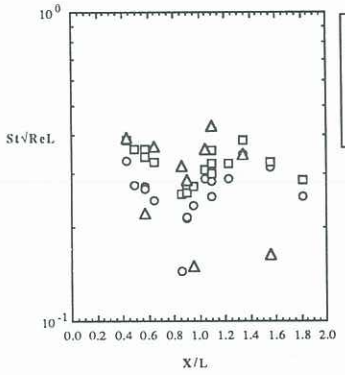

Figure 9. Heat Transfer Distribution, 5° Ramp

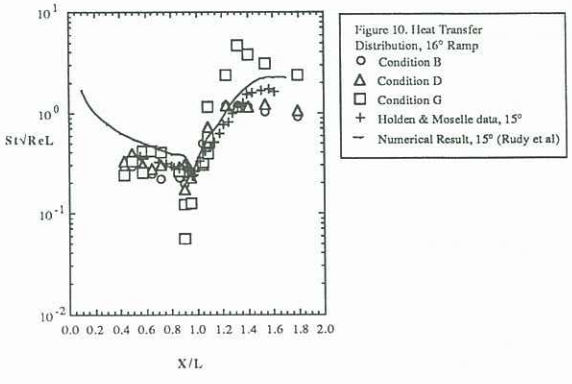

Figure 10. Heat Transfer Distribution, 16° Ramp

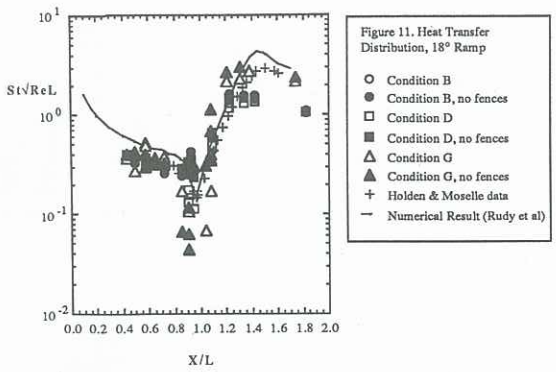

Figure 11. Heat Transfer Distribution, 18° Ramp

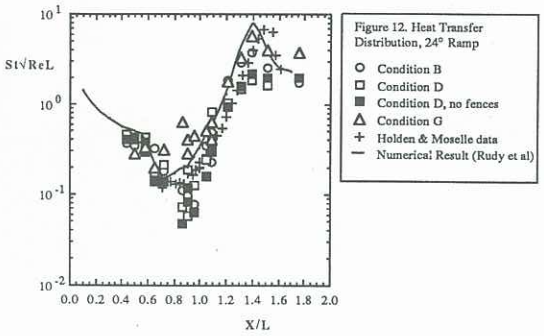

Figure 12. Heat Transfer Distribution, 24° Ramp

separated length depends inversely upon Reynolds number, it may be inferred that dissociation results in a smaller separated length. It is also clear that dissociated flows have a more diffuse reattachment process. This accords with the observations of Gai et al (1989) and Gai (1992) for high enthalpy, dissociated laminar flow over rearward facing steps.

4. CONCLUSIONS.

High enthalpy laminar flow in compression corners has been investigated. The data for zero degree compression agrees with the flat plate data of East at al(1980) which was obtained in the same facility. The flow was observed to be two-dimensional, even for the largest compression angle and for flow without side plates. The separated length was observed to be smaller in dissociated flow than in undissociated flow. This is because the dissociation reduces the boundary layer viscosity which, in turn, decreases the length of separated flow. The reattachment process is noticeably less pronounced for dissociated flows than undissociated flows, which was also observed for high enthalpy laminar flow over rearward facing steps.

Acknowledgement
The authors would like to thank P.Walsh of ANU for his assistance in operating T3.

References

Ball, KOW (1967) Wall temperature effect on incipient separation. AIAA J, 5(12), 2283-2284

Crane, KCA, Stalker, RJ (1977) Mass-spectrometric analysis of hypersonic flows. J Phys D: Appl Phys, 10(5), 679-695

East, RA, Stalker, RJ, Baird, JP (1980) Measurements of heat transfer to a flat plate in a dissociated high-enthalpy laminar air flow. J Fluid Mech, 97(4), 673-699

Gai, SL (1992) Separated high enthalpy dissociated laminar hypersonic flow behind a step-pressure measurements. AIAA J, 30(7), 1915-1918

Gai, SL, Reynolds, NT, Ross, C, Baird, JP (1989) Measurements of heat transfer in separated high-enthalpy dissociated laminar hypersonic flow behind a step. J Fluid Mech, 199, 541-561

Hanky, WL (1967) Prediction of incipient separation in shock-boundary-layer interactions. AIAA J, 5(2), 355-356

Holden, MS (1971) Establishment time of laminar separated flows. AIAA J, 9(11), 2296-2298

Holden, MS, Moselle, JR (1970) Theoretical and experimental studies of the shock wave-boundary layer interaction on compression surfaces in hypersonic flow. ARL rept ARL-70-0002

Hung, CM, MacCormack, RW (1976) Numerical solutions of supersonic and hypersonic laminar compression corner flows. AIAA J, 14(4), 475-481

Lordi, JA, Mates, RE, Moselle, JR (1966) Computer program for the numerical solution of nonequilibrium expansions of reacting gas mixtures. NACA comp rept CR-472

Mallinson, SG, Gai, SL (1992) Establishment of laminar separated flows in a free-piston shock tunnel. paper presented at IUTAM Symp on Aerothermochemistry of Re-entry Vehicles and Associated Hypersonic Flows, Marseille, France, September 1-4, 1992.

Needham, DA (1965) A heat-transfer criterion for the detection of incipient separation in hypersonic flow. AIAA J, 3(4), 781-783

Park, C (1990) Nonequilibrium Aerothermodynamics. Wiley Interscience

Rayner, JP (1973) Boundary layer separation and thermal cooling. PhD Thesis, Australian National University

Rizzetta, D, Mach, K (1989) Comparative numerical study of hypersonic compression ramp flows. AIAA paper 89-1877

Rom, J (1963) Measurements of heat transfer rates in separated regions in a shock tube and in a shock tunnel. AIAA J, 1(9), 2193-2194

Rudy, DH, Thomas, JL, Kumar, A, Gnoffo, PA, Chakravarthy, SR (1991) Computation of laminar hypersonic compression-corner flows. AIAA J, 29(7), 1108-1113

Stalker, RJ (1972) Development of a hypervelocity wind tunnel. Aeron J, 76(738) 374-384

Stalker, RJ (1985) Free-piston shock tunnel T3. Facility Handbook, University of Queensland

Stalker, RJ, Rayner, JP (1986) Shock wave-laminar boundary layer interaction at finite span compression corners. In Shock Waves and Shock Tubes, Proc 15th Int Symp on Shock Waves and Shock Tubes, Berkeley, CA, July 28-August 2 1985, D Bershader, R Hanson, eds., Stanford University Press, 509-515